IMA Journal of Mathematics Applied in Medicine & Biology (1993) **10**, 83–95

Chaos and complexity in measles models: A comparative numerical study

BENJAMIN BOLKER

Department of Zoology, Cambridge University, Downing Street, Cambridge CB2 3EJ, UK

[Received 6 July 1992 and in revised form 12 February 1993]

Recurrent epidemics of measles in developed countries offer a proving ground for current theories of complicated dynamics in ecological and epidemiological systems. This paper contrasts the basic forced SEIR model for measles with a variety of more complicated and realistic models, showing that variations in seasonal forcing and age-structured mixing patterns can generate a wide range of global dynamics. The well-known chaotic dynamics of the forced SEIR model appear to be absent from more realistic models, suppressed by the buffering effect of a low-risk group of pre-school children. These results, and the variety of measles dynamics seen in real populations with different demographic and geographic patterns, point out the need for age- and spatially-structured measles models and suggest caution in the construction of models for complicated systems.

Keywords: chaos; measles; models; age structure; seasonality; complexity; simulation.

1. Introduction

The dynamics of measles in the human populations of developed countries have generated two large bodies of modelling analysis, from the perspectives of epidemiology and of ecological dynamics. Measles was a serious public health problem in developed countries before the advent of mass vaccination programmes (Anderson, 1982) and continues to kill more than a million children per year in developing countries (Mclean, 1986).

Epidemiologists have explored the dynamics of childhood diseases in general and measles in particular in great detail, with some success. A large quantitative literature explores the dynamic effects of different vaccination strategies on age-structured models, including such realistic complexities as different mixing patterns and maternal immunity (Anderson & May, 1983, 1985; Hethcote, 1988; Tudor, 1985; Greenhalgh, 1988a, b).

Researchers in ecological dynamics, on the other hand, have focused on the irregular recurring epidemics occurring at periods of two to four years in large cities such as Copenhagen and New York City (Sugihara & May, 1990; Schaffer & Kot, 1985; Olsen *et al.*, 1988; Olsen & Schaffer, 1990; Sugihara *et al.*, 1990; Rand & Wilson, 1991; Nychka *et al.*, 1992). These cycles are caused by exhaustion and subsequent build-up of susceptibles in the population and are kept going by seasonal changes

in virus transmission. Although epidemics are more regular in some places, for example England and Wales, the measles host–microparasite system is still one of the best candidates for chaotic dynamics in an ecological system (Schaffer, 1985; Schaffer & Kot, 1985).

The simplest measles model, the seasonally forced SEIR model (Schwartz, 1985; Smith, 1982b; Schwartz & Smith, 1983; Aron & Schwartz, 1984), generates an extremely rich spectrum of dynamical behaviour, but the behaviour of this simple homogeneous system is sensitive to added heterogeneity in the system; more biologically realistic models can suppress chaotic dynamics (Bolker & Grenfell, 1993). Conclusions from these realistic models bear strongly on important general questions of heterogeneity, persistence, and chaos in ecological and epidemiological systems.

This paper gives a formal structure for a family of deterministic models that spans the sinusoidally forced SEIR and a realistic age-structured (RAS) model (Schenzle, 1984), from the simplest to the most biologically complex measles model currently present in the literature. The paper defines a general class of measles models, describes the SEIR and RAS model in terms of the general definition, and specifies a two-dimensional (age structure × seasonal pattern) family of models interpolating between the SEIR and RAS models. This family of models shows a range of dynamics from large-amplitude chaos to regular biennial patterns; the paper explores and attempts to explain varying dynamics in terms of epidemiological mechanisms.

2. Basic epidemiology of measles

The natural history of measles infections is relatively simple (Black, 1984), lending itself to straightforward compartmental modelling. Strain variation is minimal, carrier states rare or absent, and immunity is lifelong in immunocompetent individuals (Black, 1984). Children are born *susceptible*, after a 6–9 month period of neonatal immunity (Black, 1984). When virus is transferred from an infectious individual, usually by aerosol particles, susceptible children become *exposed* or latent for 6–9 days, after which they are *infective*, capable of transmitting the disease to others, for 6–7 days; clinical symptoms of rash and fever appear about 5 days into the infectious period. After measles runs its course, individuals gain lifelong immunity, effectively leaving the epidemiological system.

The most familiar mathematical formulation of these epidemiological facts is the SEIR (susceptible/exposed/infective/recovered) model, which divides the population into these categories, assuming that the population is otherwise homogeneous, and represents the flow of individuals through successive compartments by ordinary differential equations (ODEs). Recent extensions of the SEIR model have included heterogeneities in terms of age (Tudor, 1985; Anderson & May, 1985; Schenzle, 1984; Greenhalgh, 1987, 1988a, b; Hethcote, 1988; Griffiths, 1974; Dietz & Schenzle, 1985), seasonality (Aron & Schwartz, 1984; Schwartz & Smith, 1983; Schwartz, 1985, 1992; Smith, 1982b; Schenzle, 1984), and spatial structure (Bartlett, 1957, 1960; Murray & Cliff, 1975; Schwartz, 1992).

3. Measles models

3.1 *General model*

A general partial differential equation (PDE) model which encompasses a variety of the models in the literature and gives a formal structure for exploring the dynamical effects of various heterogeneities is given below. It captures the basic features of measles epidemiology discussed above and allows for differences in transmission according to age and season. This model extends the formulation given by May (1986) by making the *force of infection* λ a function of both age a and time t. As discussed by Anderson & May (1983), the combined derivative $(\partial/\partial t + \partial/\partial a)$ simply represents the fact that individuals continuously change in both age and epidemiological status, and that they age at the same rate at which time passes. With enough simplification or computational power, these equations can be integrated over age to give equilibrium solutions of the epidemiological age structure of the population, or integrated over time to give time-dependent epidemic curves. The equations are

$$\left.\begin{aligned} \frac{\partial S}{\partial t} + \frac{\partial S}{\partial a} &= -[\lambda(a,t) + \mu(a)]S(a,t), \\ \frac{\partial E}{\partial t} + \frac{\partial E}{\partial a} &= \lambda(a,t)S - [\mu(a) + \sigma]E(a,t), \\ \frac{\partial I}{\partial t} + \frac{\partial I}{\partial a} &= \sigma E - [\mu(a) + \gamma]I(a,t), \\ S + E + I + R &= N, \end{aligned}\right\} \tag{1}$$

where the differential equation for recovered individuals (R) is redundant since the total population N remains constant. The boundary conditions are

$$S(0,t) = \nu = N/L, \qquad E(0,t) = I(0,t) = 0, \tag{2}$$

where L is the average lifespan, and the initial conditions are

$$S(a,0) = S_0(a), \qquad E(a,0) = E_0(a), \qquad I(a,0) = I_0(a). \tag{3}$$

For simulation, the easiest strategy is to set the initial conditions (S_0, E_0, I_0) to their nonseasonal equilibrium values, calculated from a time-independent $\lambda(a,t) = \lambda'(a)$ (see below), and to discard the transient dynamics until several generations of hosts have passed through the system.

In these equations per capita death rate, disease incubation and infectious periods, and gross birth rate are $\mu(a)$, $1/\sigma$ and $1/\gamma$, and ν respectively. The model assumes a constant population size, no disease-induced mortality, neither neonatal immunity nor vaccination, and constant exponential distributions of lifespan and latent and infective periods. Other work has relaxed these assumptions in various contexts (May, 1986; Mclean & Anderson, 1988a, b; Grossman, 1980; Hoppensteadt, 1974; London & Yorke, 1973), but they will not be discussed further here.

The key parameter of the model is the *force of infection* $\lambda(a, t)$, which incorporates all information about age structure and seasonal variations in transmission rates. The general form of λ is an integral over age of *contact rate* β times infectives. Infectives of age a' meet and transmit disease to susceptibles of age a at a rate depending on the time of year:

$$\lambda(a, t) = \int_0^L \beta(a, a', t) I(a')\, da'. \tag{4}$$

In practice, individuals fall into C discrete *age classes* $(c_1, ..., c_C)$, with a base contact rate $\beta_{ij,0}$ between susceptibles in class i and infectives in class j. Seasonal changes in contact rate are governed by an annually periodic function $f_{\text{seas}}(t)$ that ranges from 0 to 1, and by the age-dependent amplitudes $\beta_{ij,\Delta}$, expressed as differences between minimum and maximum contact rates. The resulting expression for λ is

$$\lambda_i(t) = \sum_{j=1}^{C} \left((\beta_{ij,0} + f_{\text{seas}}(t) \times \beta_{ij,\Delta}) \times \int_{a' \in c_j} I(a')\, da' \right). \tag{5}$$

Numerical solutions This seasonal, age-structured model, while general, is intractable analytically. Epidemiologists, with an important exception (Schenzle, 1984: see below), generally simplify the model by ignoring seasonality; this omission allows them to estimate the equilibrium parameters from data. Dynamicists, on the other hand, tend to ignore age structure, which would clutter their simple nonlinear models. In practice, numerical simulations can retain the mechanisms of seasonality, age structure, and their interaction, and draw novel conclusions. These models show that seasonality is epidemiologically important, affecting persistence; that age structure is dynamically important, inhibiting chaos; and that the interaction of seasonality and age structure causes surprising changes in model dynamics.

In practice the age-structured models integrate discrete approximations of the PDEs; the analogous system of age-independent equations uses ODEs. A particular variant suggested by Schenzle (1984) uses 'coarse-grained' PDEs: that is, instead of attempting to use age compartments sufficiently small to approximate a differential age class da, it uses one-year age compartments Δa reflecting the annual cohort structure of schools.

3.2 *Sinusoidally forced SEIR model*

The model structure given above is sufficiently flexible to incorporate simple models. The familiar seasonally driven SEIR model used in many analyses of measles dynamics can be written as a special, single-age-class, case of the general model, as follows:

$$\beta_{ij,\min} = b_1 \qquad (= \beta_0(1 - \beta_1), \tag{6}$$

$$\beta_{ij,\Delta} = b_2 \qquad (= 2\beta_0\beta_1). \tag{7}$$

The parameters are also given in brackets in terms of the more familiar model formulation where β_0 represents the average contact rate and β_1 is the proportional amplitude of seasonal change in contact rate. The seasonal forcing and mortality

patterns are

$$f_{\text{seas}}(t) = \tfrac{1}{2}(1 + \cos 2\pi t) \tag{8}$$

$$\mu(a) = \mu'. \tag{9}$$

Large values of b_2, the annual swing in contact rate, generate extremely rich dynamical structures (Fig. 1a). These structures, among them bifurcation routes to chaos, fractal domain boundaries, and chaotic repellors, and their possible relevance for forecasting and control of epidemics, have been extensively discussed in the literature (Sugihara *et al.*, 1990; Schaffer *et al.*, 1993; Schaffer & Kot, 1985; Schwartz, 1985; Schwartz & Smith, 1983; Rand & Wilson, 1991) and will not be covered further here.

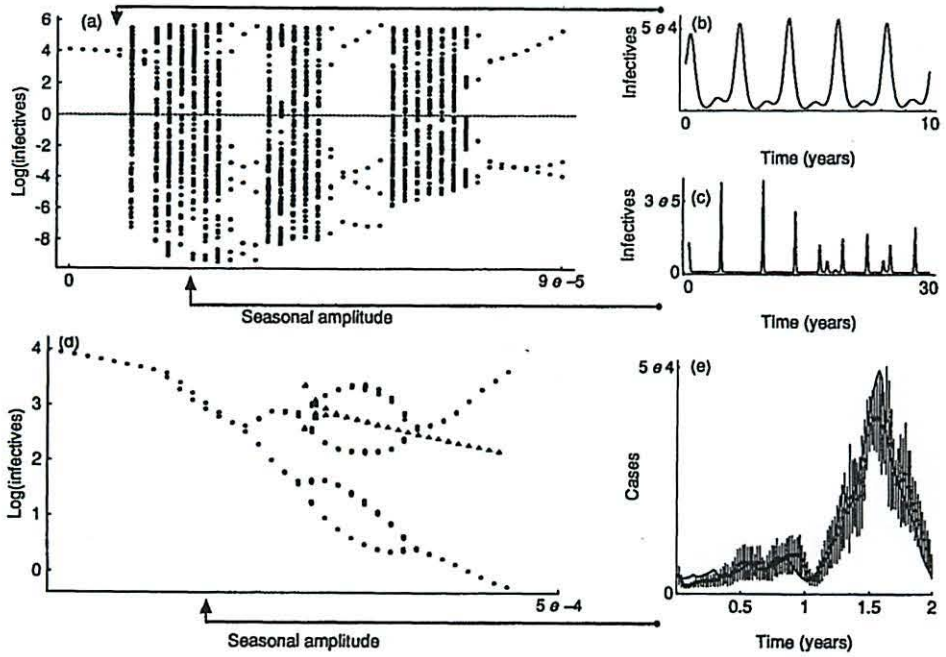

FIG. 1. Output of sinusoidally forced SEIR and realistic age-structured (RAS) models: bifurcation diagrams (a, d) and numbers of infectives over time (b, c, e). Bifurcation diagrams show Poincaré sections of $\log_{10}$ (infectives) in a population of 50 million, sampled annually at the beginning of the epidemiologic year (September, near the minimum number of infectives) for 100 years after a 200-year transient, for given values of seasonal forcing amplitude. (a) Sinusoidal SEIR bifurcation diagram, $\log_{10}$ (infectives) vs. b_2 (parameters $N = 5 \times 10^7$, $\mu = 0.02$, $\sigma = 45.6$, $\gamma = 73.0$, $b_1 = 1.5 \times 10^{-5}$, $b_2 = 0$ to 9.0×10^{-5}, all units year^{-1} except contact rate (year^{-1} infective^{-1})). (b) SEIR infectives vs. time for the biennial regime, $b_2 = 8.5 \times 10^{-6}$. (c) SEIR infectives vs. time for the chaotic regime, $b_2 = 2.0 \times 10^{-5}$. (d) Bifurcation diagram for the RAS model as described above. Parameters as given by Schenzle (1984): $N = 5 \times 10^7$, $\mu = 0.018$, birth rate = 666666, $\gamma = 73.0$, $\sigma = 45.6$ (year^{-1}). Contact rates adjusted to give best least-squares fit to the England and Wales data (Fig. 2e): $b_1 = 8.76 \times 10^{-6}$, $b_2 = 0$ to 5×10^{-4}, $b_3 = 2.74 \times 10^{-6}$, $b_4 = 4.38 \times 10^{-6}$ (year^{-1} infective^{-1})). Triangular points at large amplitudes indicate a coexisting dynamical domain in phase space. (e) RAS infectives vs. time and weekly case reports for contact rate parameters ($b_1 = 8.76 \times 10^{-6}$, $b_2 = 1.25 \times 10^{-4}$) giving best least-squares fit to case reporting data for England and Wales. The means $\pm$ one standard deviation for the (corrected) (Fine & Clarkson, 1982) weekly case reports from England and Wales, 1950–1964, are superimposed on one biennium of model output.

3.3 *Age-structured models: realistic age-structured (RAS) model*

At the other end of the spectrum of complexity, the general model can accommodate quite detailed models. Researchers have thoroughly explored nonseasonal, age-structured ($\beta_{ij,\Delta} = 0$) models, examining among other topics the impact of different age structures on eradication thresholds and optimal vaccination strategies. Schenzle, however, has contributed the only known *seasonal* age-structured model. The baseline age-structure matrix is

$$\beta_{ij,0} = \begin{bmatrix} b_1 + b_3 + b_4 & b_1 + b_3 + b_4 & b_3 + b_4 & b_4 \\ b_1 + b_3 + b_4 & b_1 + b_3 + b_4 & b_3 + b_4 & b_4 \\ b_3 + b_4 & b_3 + b_4 & b_3 + b_4 & b_4 \\ b_4 & b_4 & b_4 & b_4 \end{bmatrix}, \tag{10}$$

with $(c_1 = (0 \leqslant a < 6), c_2 = (6 \leqslant a < 10), c_3 = (10 \leqslant a < 20), c_4 = (a \geqslant 20))$, reflecting the general observation that force of infection is highest among pre- and primary-school children (Grenfell & Anderson, 1985).

The seasonal pattern reflects the observations that seasonal changes in contact rate are closely linked to school calendars (Fine & Clarkson, 1982), and that primary school children experience a sharp rise in force of infection:

$$\beta_{ij,\Delta} = \begin{bmatrix} 0 & 0 & 0 & 0 \\ 0 & b_2 & 0 & 0 \\ 0 & 0 & 0 & 0 \\ 0 & 0 & 0 & 0 \end{bmatrix}, \tag{11}$$

$$f_{\text{seas}}(t) = \begin{cases} 0 & \text{vacation,} \\ 1 & \text{school term.} \end{cases} \tag{12}$$

The structure of the parameters in the β matrices makes it possible to estimate the parameters $b_1 - b_4$ from serological or age-structured case reporting data; in general data show $b_2 > b_1 > b_3 > b_4$ (Grenfell & Anderson, 1985). We make the approximation that $f_{\text{seas}} \equiv 1$, following Schenzle (1984); in practice f_{seas} should be set to a constant value reflecting the fraction of time primary children spend in school ($\approx 2/3$) (Garnett, 1990), but in any case we usually use the estimated b values as a starting point for least-squares fits of the aggregate number of infectives over time to case reports from England and Wales.

Finally, the mortality structure approximates that of developed countries (May, 1986):

$$\mu(a) = \begin{cases} 0 & (a \leqslant 20), \\ \mu' & (a > 20). \end{cases} \tag{13}$$

As noted above, the PDEs are coarsely grained so that children move through the system in annual cohorts to simulate the movement of school classes. The RAS model

provides a better fit to the observed pattern of case reports in England and Wales than does the SEIR model (compare Fig. 1b, c and Fig. 1e).

4. Numerical survey

4.1 *Qualitative global dynamics: models*

The surprising feature of Schenzle's RAS model is that—in contrast to the sinusoidal SEIR model (Fig. 1a)—its biological complexity suppresses deterministic chaos, leading to biennial or at most 4-year cyclic patterns for a wide range of primary-school contact rates (Fig. 1d), and for realistic ranges of pre-school contact rates.

Unfortunately, the RAS model has *two* major structural differences from the SEIR model—seasonality and age structure—making it hard to specify which change is making the difference in dynamics. The general model framework stated above allows us systematically to disentangle the differences between the structure and dynamics of the sinusoidal SEIR and RAS models. On the one hand, the SEIR model has a sinusoidal forcing component ($f_{\text{seas}} = f \sin 2\pi t$), homogeneous mixing ($C = 1$), and chaos; on the other, the RAS model has a realistic, binary forcing term ($f_{\text{seas}} = 0$ or 1), age structure ($C = 4$), and no chaos. A comparative survey of measles models intermediate between the RAS and SEIR models in terms of both age structure and seasonal forcing shows that, within this family of models, *both* realistic seasonal forcing and age structure are necessary to suppress chaos (Fig. 2).

As noted above, the models use ODEs in homogeneous ($C = 1$) models and PDEs in age-structured ($C > 1$) models. The comparative study uses fine-grained ($da = 2.3$ days) instead of coarse-grained ($da = 1$ year) PDEs to avoid the confounding effect of discrete cohort advancement in the RAS model. The annual shocks of cohort advancement make the dynamics of the RAS model more (Fig. 1d), rather than less (Fig. 2d), complicated. Age structure varies by the number of age classes ($C = 1, 2, 4$), preserving as much as possible the basic structure of high, seasonally varying contact rates in one group surrounded by low, constant contact rates in all other groups. The β matrices for the two-age-class case are

$$\beta_{ij,\min} = \begin{bmatrix} b_1 & b_1 \\ b_1 & b_1 \end{bmatrix}, \qquad \beta_{ij,\Delta} = \begin{bmatrix} 0 & 0 \\ 0 & b_2 \end{bmatrix}, \tag{14}$$

$c_1 = (0 \leqslant a < 6)$, $c_2 = (a > 6)$; those for the one- and four-age-class models are as given above for the RAS and SEIR models.

The pattern of seasonal forcing varies from a simple sine wave, as given for the SEIR model; to a more realistic but still basically sinusoidal pattern fitting the annual pattern in seasonality estimated from New York City data,

$$f_{\text{seas}}(t) = 2.71739 \times \left(\frac{2.02 + 1.5 \cos 2\pi t}{1.5 + \cos 2\pi t} - 1.04 \right) \tag{15}$$

(modified from Kot *et al.*, 1988); to a simple binary pattern

$$f_{\text{seas}}(t) = \begin{cases} 0 & \text{if } 182 \leqslant (365 \times (t - [t])) \leqslant 268, \\ 1 & \text{otherwise,} \end{cases} \tag{16}$$

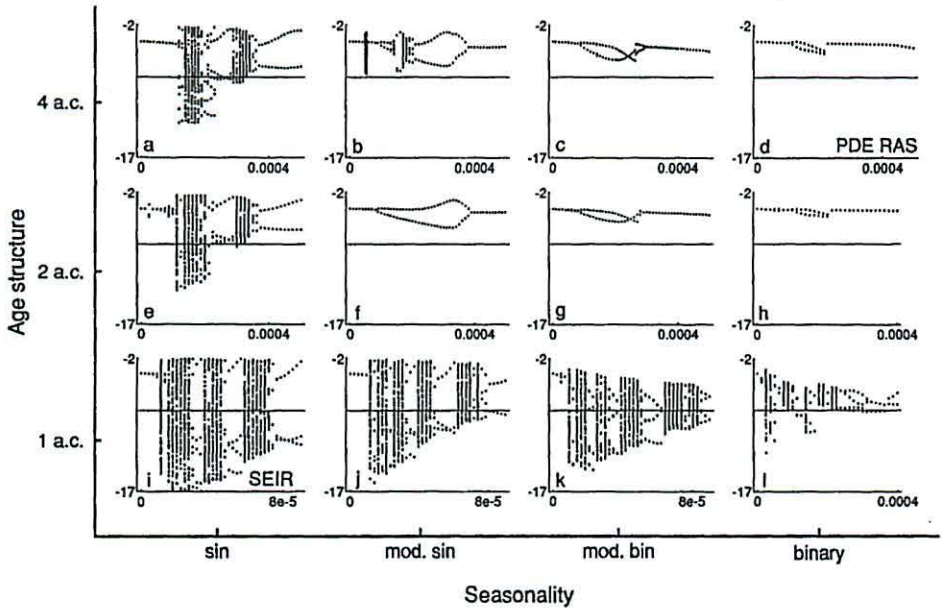

FIG. 2. Bifurcation diagrams of the family of deterministic models. Individual plots show Poincaré sections of $\log_{10}$ (fraction infective) near the epidemic minimum for different values of the seasonal forcing parameter, as described in Fig. 1. The models are arranged by complexity of age structure and seasonal forcing pattern. The horizontal axis shows increasing complexity in seasonal forcing pattern f_{seas}, as given in equations (8), (15), (16), (12) respectively; the vertical axis shows increasing complexity in age-structure matrices β, as given in equations (6, 7), (14), (10, 11). Figure 2i represents the sinusoidal SEIR model and Fig. 2d a version of the RAS model without discrete cohorts. The horizontal line in each sub-figure indicates a fractional level of one infective per 50 million population, the lower limit of a real system or discrete stochastic model in a population the size of England and Wales.

where $[t]$ is the largest integer less than or equal to t—giving the same number of vacation days as the RAS calendar in one continuous 'vacation' in the middle of the year; to the realistic school-term pattern used in the RAS model, given by Schenzle (1984).

4.2 *Qualitative global dynamics: results*

Figure 2 shows the results of numerical simulations of the family of models discussed above, showing the effects of varying the degree of biological complexity in terms of either age structure or the seasonal pattern of changes in contact rate. The parameters are chosen from the literature in a way that attempts to make different models as comparable as possible. The figure shows the qualitative global dynamics for each model—that is, whether the numerical solutions show stability, periodicity, or chaos—over a wide range of seasonal forcing amplitude, the parameter that generates a bifurcation route to chaos in the sinusoidal SEIR model (Fig. 1a).

Bifurcation diagrams show the Poincaré section of the logged fraction of infectives in the population against the amplitude of seasonal forcing, indicating the periodicity

for each parameter value. Barring a complete exploration of the parameter and phase space of each model, which would be both computationally and graphically difficult, a broad survey of seasonal forcing over several orders of magnitude should give a reasonable estimate of whether chaos is part of the repertoire of dynamical behaviour of a model. For example, in the sinusoidally forced SEIR model, transient chaos in asymptotically stable parameter regimes is caused by the 'ghost' of chaotic structures present in other parameter regimes (Rand & Wilson, 1991).

Bifurcation diagrams do not necessarily show the entire range of dynamics for a particular model (Holden, 1986). Parameters other than seasonal forcing do affect the dynamics in independent ways, particularly b_1, the baseline child contact rate, in the RAS model. Also, multiple domains are possible in phase space (Schwartz 1985); that is, different starting values (S_0, E_0, I_0) may lead to different long-term model dynamics in certain cases (Fig. 1d). Nevertheless, the bifurcation diagram gives a good general synopsis of the comparative degree of irregularity and chaos in the dynamics of a particular model.

Dynamical complexity and model structure The simulations show (Fig. 2) that dynamical complexity increases with decreasing age structure (Fig. 2d, h, l) *and* with decreasing complexity of seasonal forcing pattern (Fig. 2d, c, b, a). A homogeneous model incorporating the seasonal pattern of effective contact rates generated by the RAS model can generate chaos (Fig. 2l); so can an age-structured model with simple sinusoidal forcing (Fig. 2a). The main criteria for suppressing chaos in this family appear to be some degree of age structure and some seasonal pattern more complex than a simple sinusoid (Fig. 2b, c, d, f, g, h). (*Note* that f_{seas} for the homogeneous, binary model is not a true binary function; rather, it is the effective contact rate generated by the RAS model. This variant was used for closer analogy with the RAS model structure, and its dynamics resemble those of a homogeneous model with true binary seasonality.)

Dynamical complexity and trough minima Figure 2 also shows that dynamical complexity is inversely correlated with minimum numbers of infectives in the epidemic cycle: the Poincaré sections are taken at the beginning of the *epidemiologic year* (Anderson, 1982), near the annual minimum. The sub-figures are all on the same scale; the height of the solid horizontal line in each sub-figure corresponds to one infective in a population of 50 million, comparable to England and Wales. At the extremes, the SEIR model falls as low as one infective per 10^{17}, an obviously unrealistic level, while the PDE RAS model only falls to one in 10^4. With fewer than one infective in the population, measles will fail to persist; stochastic fluctuations in the infection process mean measles will sometimes fade out even with larger average numbers of infectives. Measles apparently persists in large populations (Black, 1966; Bartlett, 1957, 1960), and so deterministic models with extremely low epidemic troughs are unrealistic in a critically important way (Grenfell, 1992). Dynamical complexity appears primarily in members of the model family whose trough minima fall below a realistic level (Fig. 2a, e, i, j, k, l).

Chaos in the SEIR model is associated with the deep troughs between epidemics (Drepper, 1988); adding a large enough immigration of infectives suppresses chaos in

the SEIR model. Berryman & Millstein (1989) suggest that large-amplitude fluctuations around an equilibrium, causing large, overcompensating density-dependent growth rates, commonly—although not always (Nisbet *et al.*, 1989)—generate chaos. This mechanism appears to drive chaotic dynamics in measles models, and preventing low minima (and hence large growth rates) appears to short-circuit chaos. Thus the absence of chaos in the RAS model probably comes about because pre-school children are shielded from the full force of epidemics, and so provide a trickle of infectives that prevents low minima. The role of complex seasonality is not yet clear—it may break up epidemics more effectively than sinusoidal seasonality, and thus prevent them from completely exhausting the number of susceptibles. The minor epidemic in the RAS biennial regime ends because vacation disperses children rather than because the supply of susceptibles is exhausted (Schenzle, 1984), and binary seasonality may contribute to this effect.

5. Discussion and Conclusions

The general model presented here is a unifying strategy for looking at a variety of measles models that generates a range of dynamics from simple to complex. The numerical survey of dynamics within this family shows convincingly that, in this family of epidemiological models, model complexity, trough minima, and dynamic simplicity are correlated. This correlation proves no causal links, but simple epidemiological and dynamical arguments suggest that biological heterogeneities cause a buffering effect that prevents unrealistically low interepidemic troughs and thus damps out chaotic dynamics in the models.

This framework offers one possibility for unifying the irregular and possibly chaotic measles epidemics of Copenhagen and New York City (Sugihara & May, 1990; Schaffer & Kot, 1985; Olsen *et al.*, 1988; Olsen & Schaffer, 1990; Sugihara *et al.*, 1990; May *et al.*, 1992; Drepper, 1988; Stollenwerk & Drepper, 1993; Nychka *et al.*, 1992; Casdagli, 1992) and the regular biennial epidemics of England and Wales within a single framework by varying the type of age structure and seasonal pattern. Plausible local differences in school calendar, age at school attendance, and mixing between pre-school and primary-school children could generate differences in seasonal patterns and age structure that qualitatively change epidemic dynamics. While this explanation is more general than simply assuming that dynamics vary from place to place because of differences in seasonal amplitude, many unanswered questions remain about the dynamics of measles models, particularly about the effects of population size and geographic and social coupling between different populations.

The importance of trough minima points to the importance of population size in measles dynamics. Preliminary results from discrete stochastic analogues (Murray & Cliff, 1975; Olson *et al.*, 1988) of the RAS and SEIR models suggest an important dynamical effect of population size. Although most of the dynamical differences between the SEIR and RAS models carry over from deterministic to simple stochastic models, different-size populations generate different dynamics in the Monte Carlo RAS model: at large ($N = 5 \times 10^7$) population sizes, the RAS model approximates its deterministic analogue and generates a fairly stable biennial pattern, while at smaller population sizes ($N = 10^6$), it generates episodic dynamics alternating

between an irregular, fadeout-dominated triennial pattern and a more predictable biennial pattern (Bolker & Grenfell, 1993). These distinct dynamical domains also appear in the stochastic SEIR and in the deterministic SEIR model, where they correspond to different regions of the complex underlying deterministic (chaotic) attractor structure (Schaffer *et al.*, 1993).

These results are discussed elsewhere (Bolker & Grenfell, 1993); the main conclusion from the current study is that detailed consideration of social and biological complexities is vital. Particular patterns of heterogeneity in seasonal and age structure can have profound effects on the dynamics of epidemiological models, and complex models should not be dismissed in favour of simpler ones without first exploring their dynamical behaviour.

Acknowledgements

I would like to thank Bryan Grenfell for a great deal of useful advice and guidance, Darren Shaw, Adam Kleczkowski, and Howard Wilson for useful suggestions, and the Paul Mellon Fellowship for financial support.

This paper is based on an article read at the Sixth IMA Conference on the Mathematical Theory of the Dynamics of Biological Systems, held in Oxford, 1–3 July 1992.

References

ANDERSON, R. M. 1982 Directly transmitted viral and bacterial infections of man. In: *Population Dynamics of Infectious Diseases: Theory and Applications* (R. M. Anderson, ed.), pp. 1–37. London: Chapman & Hall.

ANDERSON, R. M., & MAY, R. M. 1983 Vaccination against rubella and measles: Quantitative investigations of different policies. *J. Hyg.* (*Camb.*) **90**, 259–325.

ANDERSON, R. M., & MAY, R. M. 1985 Age-related changes in the rate of disease transmission: Implications for the design of vaccination programmes. *J. Hyg.* (*Camb.*) **94**, 365–436.

ARON, J. L., & SCHWARTZ, I. B. 1984 Seasonality and period-doubling bifurcations in an epidemic model. *J. Theor. Biol.* **110**, 665–79.

BARTLETT, M. S. 1957 Measles periodicity and community size. *J. R. Statist. Soc.* A **120**, 48–70.

BARTLETT, M. S. 1960 The critical community size for measles in the U.S. *J. R. Statist. Soc.* A **123**, 37–44.

BERRYMAN, A. A., & MILLSTEIN, J. A. 1989 Are ecological systems chaotic—and if not, why not? *TREE* **4**, 26–8.

BLACK, F. L. 1966 Measles endemicity in insular populations: Critical community size and its evolutionary implication. *J. Theor. Biol.* **11**, 207–11.

BLACK, F. L. 1984 Measles. In: *Viral Infections of Humans: Epidemiology and Control* (A. S. Evans, ed.), pp. 397–418. New York: Plenum.

BOLKER, B. M., & GRENFELL, B. T. 1993 Chaos and biological complexity in measles dynamics. *Proc. R. Soc. London. Biol.* **251**, 75–81.

CASDAGLI, M. 1992 Chaos and deterministic versus stochastic nonlinear modeling. *J. R. Statist. Soc.* B **54**, 303–28.

DIETZ, K., & SCHENZLE, D. 1985 Mathematical models for infectious disease statistics. In: *A Celebration of Statistics* (A. C. Atkinson & S. E. Feinberg, eds.), pp. 167–204. New York: Springer.

DREPPER, F. R. 1988 Unstable determinism in the information production profile of an epidemiological time series. In: *Ecodynamics: Contributions to Theoretical Ecology* (W. Wolff, C.-J. Soeder, & F. R. Drepper, eds.), pp. 319–32. London: Springer.

FINE, P. E. M., & CLARKSON, J. A. 1982 Measles in England and Wales—I: An analysis of factors underlying seasonal patterns. *Int. J. Epidemiol.* **11**, 5–15.

GARNETT, G. P. 1990 The population dynamics of *varicella-zoster* virus. Ph.D. thesis, Sheffield University.

GRENHALGH, D. 1987 Analytical results on the stability of age-structured recurrent epidemic models. *IMA J. Math. Appl. Med. Biol.* **4**, 109–44.

GREENHALGH, D. 1988a Threshold and stability results for an epidemic model with an age-structured meeting rate. *IMA J. Math. Appl. Med. Biol.* **5**, 81–100.

GRENHALGH, D. 1988b Analytical threshold and stability results on age-structured epidemic models with vaccination. *Theor. Popul. Biol.* **33**, 266–90.

GRENFELL, B. T. 1992 Chance and chaos in measles dynamics. *J. R. Statist. Soc.* B **54**, 383–98.

GRENFELL, B. T., & ANDERSON, R. M. 1985 The estimation of age-related rates of infection from case notifications and serological data. *J. Hyg. (Camb.)* **95**, 419–36.

GRIFFITHS, D. A. 1974 A catalytic model of infection for measles. *Appl. Statist.* **23**, 330–9.

GROSSMAN, Z. 1980 Oscillatory phenomena in a model of infectious diseases. *Theor. Popul. Biol.* **18**, 204–43.

HETHCOTE, H. W. 1988 Optimal ages of vaccination for measles. *Math. Biosci.* **89**, 29–52.

HOLDEN, A. V. 1986 *Chaos.* Princeton University Press.

HOPPENSTEADT, F. C. 1974 An age dependent epidemic model. *J. Franklin Inst.* **297**, 325–33.

KOT, M., GRASER, D. J., TRUTY, G. L., SCHAFFER, W. M., & OLSEN, L. F. 1988 Changing criteria for imposing order. *Ecol. Modelling.* **43**, 75–110.

LONDON, W. P., & YORKE, J. A. 1973 Recurrent outbreaks of measles, chickenpox and mumps. I. Seasonal variation in contact rates. *Am. J. Epidemiol.* **98**, 453–68.

MAY, R. M. 1986 Population biology of microparasitic infections. In: *Biomathematics*, Vol. 17 (T. G. Hallam, & S. A. Levin, eds.), pp. 405–42. Berlin: Springer.

MAY, R. M., ISHAM, V., BOLKER, B., *et al.* 1992 Royal Statistical Society meeting on chaos—discussion. *J. R. Statist. Soc.* B **54**, 451–474.

MCLEAN, A. R. 1986 Dynamics of childhood infections in high birthrate countries. *Lecture Notes in Biomathematics 65*, pp. 171–97. Berlin: Springer.

MCLEAN, A. R., & ANDERSON, R. M. 1988a Measles in developing countries. Part II. The predicted impact of mass vaccination. *Epidemiol. Infect.* **100**, 419–42.

MCLEAN, A. R., & ANDERSON, R. M. 1988b Measles in developing countries. Part I. Epidemiological parameters and patterns. *Epidemiol. Infect.* **100**, 111–33.

MURRAY, G. D., & CLIFF, A. D. 1975 A stochastic model for measles epidemics in a multi-region setting. *Inst. Brit. Geog.* **2**, 158–74.

NISBET, R., BLYTHE, S., GURNEY, B., *et al.* 1989 Responses to Berryman and Millstein, 'Are ecological systems chaotic—and if not, why not?'. *TREE* **4**, 238–40.

NYCHKA, D., ELLNER, S., GALLANT, A. R., & MCCAFFREY, D. 1992 Finding chaos in noisy systems. *J. R. Statist. Soc.* B **54**, 399–426.

OLSEN, L. F., & SCHAFFER, W. M. 1990 Chaos versus noisy periodicity: Alternative hypotheses for childhood epidemics. *Science* **249**, 499–504.

OLSEN, L. F., TRUTY, G. L., & SCHAFFER, W. M. 1988 Oscillations and chaos in epidemics: A nonlinear dynamic study of six childhood diseases in Copenhagen, Denmark. *Theor. Popul. Biol.* **33**, 344–70.

RAND, D. A., & WILSON, H. 1991 Chaotic stochasticity: A ubiquitous source of unpredictability in epidemics. *Proc. R. Soc. Lond. Biol.* **246**, 179–84.

SCHAFFER, W. M. 1985 Can nonlinear dynamics elucidate mechanisms in ecology and epidemiology? *IMA J. Math. Appl. Med. Biol.* **2**, 221–252.

SCHAFFER, W. M., KENDALL, B. E., & TIDD, C. W. 1993 Transient periodicity and episodic predictability in biological dynamics. *Proc. R. Soc. Lond. Biol.*, submitted.

SCHAFFER, W. M., & KOT, M. 1985 Nearly one dimensional dynamics in an epidemic. *J. Theor. Biol.* **112**, 403–27.

SCHENZLE, D. 1984 An age-structured model of pre- and post-vaccination measles transmission. *IMA J. Math. Appl. Med. Biol.* **1**, 169–91.

SCHWARTZ, I. B. 1985 Multiple recurrent outbreaks and predictability in seasonally forced nonlinear epidemic models. *J. Math. Biol.* **21**, 347–61.

SCHWARTZ, I. B. 1992 Small amplitude, long period outbreaks in seasonally driven epidemics. *J. Math. Biol.* **30**, 473–91.

SCHWARTZ, I. B., & SMITH, H. L. 1983 Infinite subharmonic bifurcation in an SEIR model. *J. Math. Biol.* **18**, 233–53.

SMITH, H. L. 1982a Subharmonic bifurcation in an SIR epidemic model. *J. Math. Biol.* **17**, 163–77.

SMITH, H. L. 1982b Multiple stable subharmonics for a periodic epidemic model. *J. Math. Biol.* **17**, 179–90.

STOLLENWERK, F., & DREPPER, F. R. 1993 Evidence for deterministic chaos in empirical population fluctuations. In: *State of the Art in Ecological Modelling*, Conference Proceedings, Kiel, Germany, Oct. 1992.

SUGIHARA, G., GRENFELL, B., & MAY, R. M. 1990 Distinguishing error from chaos in ecological time series. *Phil. Trans. R. Soc. Lond. Biol.* **330**, 235–51.

SUGIHARA, G., & MAY, R. M. 1990 Nonlinear forecasting as a way of distinguishing chaos from measurement error in time series. *Nature* **344**, 734–41.

TUDOR, D. W. 1985 An age-dependent epidemic model with application to measles. *Math. Biosci.* **73**, 131–47.